Organometallics 1993, 12, 3257-3263 3257

Paramagnetic Mononuclear Rhodium(II) Organometallic Complexes. X-ray Structure of $[Rh(C_6Cl_5)_2\{P(OPh)_3\}_2]$

María P. García,[*,†] M. Victoria Jiménez,[†] Luis A. Oro,[†] Fernando J. Lahoz,[†]
José M. Casas,[†] and Pablo J. Alonso[‡]

Departamento de Química Inorgánica and Departamento de Física de la Materia Condensada,
Instituto de Ciencia de Materiales de Aragón, Universidad de Zaragoza-CSIC,
50009 Zaragoza, Spain

Received March 1, 1993

The anionic complexes $[NBu_4][Rh(C_6Cl_5)_2(L_2)]$ [L_2: 1,5-cyclooctadiene (cod), 1; $\{P(OPh)_3\}_2$, 2; $(CO)_2$, 3; $(CO)(PPh_3)$, 4], obtained from the arylation of $[\{Rh(\mu\text{-}Cl)(L_2)\}_2]$ with LiC_6Cl_5, serve as precursors to a number of rhodium(II) complexes via oxidation and substitution reactions. The oxidation of 1 and 2 with chlorine gives the neutral rhodium(II) compounds $[Rh(C_6Cl_5)_2(L_2)]$ [L_2 = cod, $\{P(OPh)_3\}_2$]. Substitution of cod in $[Rh(C_6Cl_5)_2(cod)]$ by neutral ligands, such as $P(OMe)_3$, PPh_3, pyridine (py), 1,2-bis(diphenylphosphino)ethane (dpe), and bis(diphenylphosphino)methane (dpm), renders five new neutral rhodium(II) monomer complexes. The compounds have been studied and characterized by IR, NMR, MS, EPR, and CV, and $[Rh(C_6Cl_5)_2\{P(OPh)_3\}_2]$ (6) has been structurally characterized by an X-ray diffraction study. Compound 6 crystallizes in the triclinic space group $P\bar{1}$ with $a = 9.8718(9)$ Å, $b = 11.6830(13)$ Å, $c = 12.1366(12)$ Å, $\alpha = 95.465(6)°$, $\beta = 105.824(4)°$, $\gamma = 112.738(5)°$, $V = 1209.9(2)$ Å^3, $Z = 1$ and $R = 0.041$ for 3889 observed reflections. This Rh(II) complex exhibits a centrosymmetric square-planar coordination with a *trans* arrangement of the ligands.

Introduction

Rhodium complexes with a d^7 electronic configuration are very unusual, especially as monomeric species.[1] There are relatively few reports on the coordination chemistry of paramagnetic rhodium(II)[2] and even fewer on mononuclear organometallic complexes of rhodium(II).[2,3] However, recent papers by Wayland and co-workers describing methane, toluene, and carbon monoxide activation by Rh(II) metallo radicals,[4] as well as addition of H_2 to these species,[5] make this area of research particularly attractive.

One of our current research interests is the chemistry of perhalophenyl derivatives of rhodium and iridium. We have reported a variety of neutral, anionic, mono- and di-nuclear complexes[6,7] of rhodium(III) prepared from the anionic complex[8] $[Rh(C_6F_5)_5]^{2-}$. We also recently described[9] a fully characterized monomeric square planar iridium(II) organometallic complex, $[Ir(C_6Cl_5)_2(cod)]$. The C_6Cl_5 anion stabilizes the unusual oxidation state (II) of the iridium in the same way that it does with the oxidation state (III) of platinum[10] in the complex $(NBu_4)[Pt(C_6Cl_5)_4]$. Furthermore, the use of the pentachlorophenyl ligand also provides a good route to the preparation of rhodium(II) compounds. In this paper we wish to report the synthesis of some anionic pentachlorophenyl rhodium(I) complexes, their oxidation reactions to form monomeric paramagnetic rhodium(II) complexes, and substitution reactions that allow the preparation of a variety of rhodium(II) complexes.

Results and Discussion

The anionic rhodium(I) complexes $[NBu_4][Rh(C_6Cl_5)_2(L_2)]$ [L_2: 1,5-cyclooctadiene (cod), 1; $\{P(OPh)_3\}_2$, 2; $(CO)_2$, 3; $(CO)(PPh_3)$, 4] are prepared via the addition of the solid rhodium dimers $[\{Rh(\mu\text{-}Cl)(L_2)\}_2]$ to diethyl ether solutions of LiC_6Cl_5, in an inert atmosphere at −50 °C. The lithium salt of the complexes could not be isolated, even using TMED, so compounds 1–4 are obtained as solids by the addition of a salt of a bulky cation (eq 1).

$$[\{Rh(\mu\text{-}Cl)(L_2)\}_2] + 4LiC_6Cl_5 \xrightarrow{-2LiCl} 2Li[Rh(C_6Cl_5)_2(L_2)] \rightarrow \xrightarrow[-2LiBr]{+2NBu_4Br} 2[NBu_4][Rh(C_6Cl_5)_2(L_2)] \quad (1)$$

Complex 3 is alternatively obtained by bubbling carbon monoxide through a dichloromethane solution of 1. Compounds 1–4 are stable both in the solid state, in which they can be stored for long periods, at −5 °C, without decomposition being observed, and in deoxygenated solutions, in which they behave as 1:1 electrolytes.[11] The

---

[†] Departamento de Química Inorgánica.

[‡] Departamento de Física de la Materia Condensada.

(1) Serpone, N.; Jamieson, M. A. In *Comprehensive Coordination Chemistry*; Wilkinson, G., Gillard, R. D., Mc Cleverty, J. A., Eds.; Pergamon Press: Oxford, U.K., 1987; Vol. 4, p 1120.

(2) (a) Dunbar, K. R.; Haefner, S. C.; Pence, L. E. *J. Am. Chem. Soc.* **1989**, *111*, 5504. (b) Harlow, R. L.; Thorn, D. L.; Barker, R. T.; Jones, N. L. *Inorg. Chem.* **1992**, *31*, 993. (c) Dunbar, K. R.; Haefner, S. C. *Organometallics* **1992**, *11*, 1431 and references therein.

(3) Hay-Motherwell, R. S.; Koschmieder, S. U.; Wilkinson, G.; Hussain-Bates, B.; Hursthouse, M. B. *J. Chem. Soc., Dalton Trans.* **1991**, 2821.

(4) Wayland, B. B.; Ba, S.; Sherry, A. E. *J. Am. Chem. Soc.* **1991**, *113*, 5305.

(5) Wayland, B. B.; Ba, S.; Sherry, A. E. *Inorg. Chem.* **1992**, *31*, 148.

(6) García, M. P.; Jiménez, M. V.; Lahoz, F. J.; Oro, L. A.; Tiripicchio, A.; López, J. A. *J. Chem. Soc., Dalton Trans.* **1990**, 1503.

(7) García, M. P.; Jiménez, M. V.; Oro, L. A. *J. Organomet. Chem.* **1992**, *438*, 229.

(8) García, M. P.; Oro, L. A.; Lahoz, F. J. *Angew. Chem.* **1988**, *100*, 1766; *Angew. Chem., Int. Ed. Engl.* **1988**, *27*, 12.

(9) García, M. P.; Jiménez, M. V.; Lahoz, F. J.; Oro, L. A.; Alonso, P. J. *Angew. Chem.* **1992**, *104*, 1512; *Angew. Chem., Int. Ed. Engl.* **1992**, *31*, 1527.

(10) Usón, R.; Forniés, J.; Tomás, M.; Menjón, B.; Sünkel, K.; Bau, R. *J. Chem. Soc., Chem. Commun.* **1984**, 751. Usón, R.; Forniés J.; Tomás, M.; Menjón, B.; Sünkel, K.; Bau, R.; Kuwabara, E. *Organometallics* **1986**, *5*, 1576.

(11) Geary, W. J. *Coord. Chem. Rev.* **1971**, *7*, 81.

0276-7333/93/2312-3257$04.00/0

Table I. Analyses, Yields, Colors, and Conductivities for the New Complexes

compound	anal.,[a] %			yield, %	Λ_M (C)[b]	color
	N	C	H			
$[NBu_4][Rh(C_6Cl_5)_2(cod)]$ (**1**)	1.47 (1.47)	45.43 (45.41)	5.26 (5.08)	62	94 (5.4×10^{-4})	orange
$[NBu_4][Rh(C_6Cl_5)_2\{P(OPh)_3\}_2]$ (**2**)	0.83 (0.84)	45.99 (46.18)	3.37 (3.99)	50	120 (4.8×10^{-4})	yellow
$[NBu_4][Rh(C_6Cl_5)_2(CO)_2]$ (**3**)	1.58 (1.56)	39.87 (40.03)	3.79 (4.03)	52	109 (5.0×10^{-4})	yellow
$[NBu_4][Rh(C_6Cl_5)_2(CO)(PPh_3)]$ (**4**)	1.21 (1.23)	49.57 (49.77)	4.52 (4.53)	48	99 (3.1×10^{-4})	yellow
$[Rh(C_6Cl_5)_2(cod)]$ (**5**)		33.66 (33.89)	1.50 (1.71)	62		pink
$[Rh(C_6Cl_5)_2\{P(OPh)_3\}_2]$ (**6**)		47.36 (47.17)	2.35 (2.47)	85[c]		dark pink
$[Rh(C_6Cl_5)_2\{P(OMe)_3\}_2]$ (**7**)		25.60 (25.44)	2.06 (2.13)	80		orange
$[Rh(C_6Cl_5)_2(PPh_3)_2]$ (**8**)		51.43 (51.19)	2.77 (2.68)	82		red
$[Rh(C_6Cl_5)_2(py)_2]$ (**9**)	3.54 (3.68)	34.64 (34.78)	1.20 (1.33)	48		yellow
$[Rh(C_6Cl_5)_2(dpe)]\cdot CH_2Cl_2$ (**10**)		43.22 (43.18)	2.09 (2.41)	86		pink
$[Rh(C_6Cl_5)_2(dpm)]$ (**11**)		45.35 (45.07)	2.87 (2.25)	67		brown

[a] Found (calcd). [b] Λ_M (Ω^{-1} cm^2 mol^{-1}), C (mol dm^{-3}) in acetone. [c] 48% (oxidation method of preparation).

results of the analyses, reaction yields, conductivities, and color for the new complexes are collected in Table I.

IR Spectra. All the compounds show the absorptions due to the C_6Cl_5 group[12] around 1320, 1295, 1230, 800, and 600 cm^{-1}. The band observed in the 850–820-cm^{-1} region is assigned to an X-sensitive mode involving X–C_6Cl_5 stretching and has been proved, in related derivatives of palladium and platinum, of structural interest. Only one absorption band is expected if the C_6Cl_5 groups are in *trans* positions and two if they are in mutually *cis* positions. However in our complexes only one broad band has been observed in this region, even for compound **1**, in which the *cis* configuration is required. On the other hand, the IR spectrum of compound **3** exhibits two absorptions in the carbonyl region, at 2030 and 1960 cm^{-1}, characteristic of *cis*-dicarbonylrhodium(I) complexes.[13]

NMR Spectra. The ^{1}H NMR spectra of the complexes **1**–**4** show the signals due to NBu_4^+ together with those of the neutral ligands, cod in **1**, $P(OPh)_3$ in **2**, and PPh_3 in **4**, and the integration of the signals agrees with the proposed formulation. The $^{31}P\{^1H\}$ spectra for complexes **2** and **4** show a doublet at 122.7 ppm (J_{PRh} = 239.1 Hz) and at 40.1 ppm (J_{PRh} = 131.3 Hz), respectively. The ^{13}C spectra of compounds **1**–**4** are in accordance to those expected for them; in complexes **1** and **2** the signals due to the *ipso* carbon of the C_6Cl_5 groups are not observed; for complex **4**, in the 170–200 ppm region, there are three signals: one at 195.1 ppm (dd, J_{CRh} = 62 Hz, $^3J_{CP}$ = 14 Hz), assigned to the carbon atom of the carbonyl group, and two others, corresponding to the two *ipso* carbon atoms of the C_6Cl_5 groups, at 181.4 ppm (dd, J_{CRh} = 35.5 Hz, $^3J_{CP}$ = 15.6 Hz) and at 176.4 ppm (dd, J_{CRh} = 40.5 Hz, $^3J_{CP}$ = 83.4 Hz). This shows that one of the C_6Cl_5 groups is *cis* to the P atom while the other is *trans*, so they must be in mutually *cis* positions.

Oxidation Reactions. A dichloromethane solution of **1** reacts with chlorine or iodine in a 1:1 molar ratio, at room temperature, yielding a pink solid identified as the mononuclear rhodium(II) complex $[Rh(C_6Cl_5)_2(cod)]$ (**5**). If the oxidation is carried out using silver perchlorate, the crystals of **5** have to be separated from metallic silver by differences of density.

The oxidation of **2** has been carried out with chlorine or $TlCl_3$. Treatment of an orange dichloromethane solution of **2** with an equimolar solution of Cl_2, in the same solvent, at room temperature, produces within minutes a red solution from which $[Rh(C_6Cl_5)_2\{P(OPh)_3\}_2]$ (**6**) can be isolated as a dark pink solid.

Compounds **3** and **4** also react with chlorine, but so far, we have not been able to characterize the final products. In the first case a mixture is obtained where the IR spectrum shows bands at 1705 cm^{-1} (acyl region) and at 320 cm^{-1} (ν(Rh–Cl)) and the EPR spectrum of the solid shows no signals. For complex **4**, the result of its reaction with chlorine is a compound without CO ligands. The EPR spectrum shows that the product is paramagnetic, but the signal pattern is very different from that of the other rhodium(II) complexes described in this paper. On the other hand, the reaction of **3** with $[Ph_3PAgOClO_3]$ or the reaction of **4** with $AgClO_4$ or $[Ph_3PAgOClO_3]$ gives a very unstable compound which decomposes in solution to yield the reported[14] *trans*-$[Rh(C_6Cl_5)(CO)(PPh_3)_2]$.

Substitution Reactions. An alternative route to **6** consists of the displacement of the cyclooctadiene of compound **5** by $P(OPh)_3$. Using the same synthetic method, several analogous rhodium(II) compounds of formula $[Rh(C_6Cl_5)_2L_2]$ have been prepared. When neutral ligands L are added to suspensions of **5**, in CH_2Cl_2, the solids are slowly dissolved in times from 2 to 24 h (see Experimental Section) and the resulting solutions are red, except for the case when L is pyridine (py), where the solution is yellow. Upon workup of the solutions, microcrystalline solids are isolated and identified as $[Rh(C_6Cl_5)_2L_2]$ [L_2: $\{P(OMe)_3\}_2$, **7**; $(PPh_3)_2$, **8**; $(py)_2$, **9**; 1,2-bis(diphenylphosphino)ethane (dpe), **10**; bis(diphenylphosphino)methane (dpm), **11**].

Complexes **5**–**11** have been studied and characterized by their analytical data (Table I), conductivity measure-

---

[12] Usón, R.; Forniés, J.; Martinez, F.; Tomás, M.; Reoyo, I. *Organometallics* **1983**, *2*, 1386.

[13] Khan, M. N. I.; Fackler, J. P., Jr.; Wang, J. C.; Wang, S. *Inorg. Chem.* **1988**, *27*, 1672.

[14] Royo, P.; Serrano, R. *J. Organomet. Chem.* **1978**, *144*, 33.

Table II. Formal Electrode Potentials[a] (V vs SCE) of the Redox Changes for Some of the Complexes

complex	$E^{\circ\prime}$(Rh(I)/ Rh(II))	ΔE_p,[b] V	$E^{\circ\prime}$(Rh(II)/ Rh(III))
$[Rh(C_6Cl_5)_2(cod)]^-$ (**1**)	–0.07	0.074	$E_{p,a}$ = 1.36[c]
cis-$[Rh(C_6Cl_5)_2\{P(OPh)_3\}_2]^-$ (**2**)	–0.12	0.099	
$[Rh(C_6Cl_5)_2(CO)_2]^-$ (**3**)	$E_{p,a}$ = 0.67, $E_{p,c}$ = 0.60[c]	0.074	
$[Rh(C_6Cl_5)_2(CO)(PPh_3)]^-$ (**4**)	0.10	0.066	
$[Rh(C_6Cl_5)_2(cod)]$ (**5**)	–0.07	0.070	
trans-$[Rh(C_6Cl_5)_2\{P(OPh)_3\}_2]$ (**6**)	–0.32	0.070	
$[Rh(C_6Cl_5)_2(PPh_3)_2]$ (**8**)	–0.62	0.080	
$[Rh(C_6Cl_5)_2(dpe)]$ (**10**)	–0.51	0.078	$E_{p,a}$ = 0.40, $E_{p,c}$ = –0.01[c]

[a] CH_2Cl_2 solution containing the complexes and $[NBu_4][PF_6]$ (0.1 mol·dm^{-3}); room temperature; v = 0.10 V s^{-1}; platinum electrode. [b] $E_{p,a} - E_{p,c}$ with v = 0.1 V s^{-1}. [c] Not reversible.

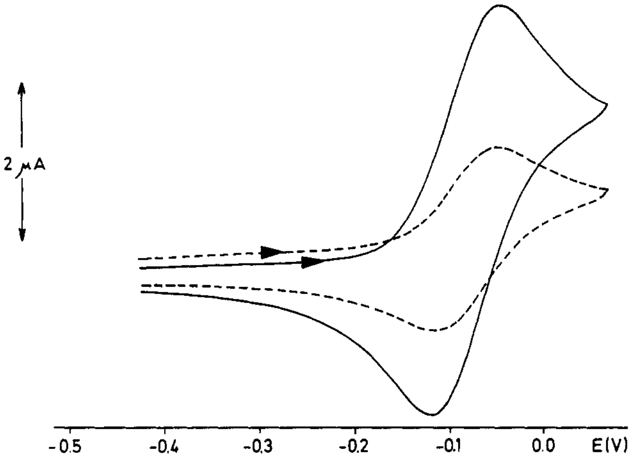

Figure 1. CV scans of $[NBu_4][Rh(C_6Cl_5)_2(cod)]$ (**1**) (0.50 mM) and $[Rh(C_6Cl_5)_2(cod)]$ (**5**) in CH_2Cl_2/0.1 M $[NBu_4][PF_6]$ at ambient temperature (v = 0.10 V s^{-1}; Pt electrode).

ments, IR, MS, EPR, and cyclic voltammetry, and one of them, **6**, has been characterized by an X-ray crystallographic study; their ^1H and ^{31}P NMR spectra are broad and essentially featureless, consistent with their formulation as paramagnetic species.

Electrochemistry. Compounds **1**–**6**, **8**, and **10** were studied by cyclic voltammetry. In all the cases the experiments were carried out in CH_2Cl_2 employing Bu_4NPF_6 as the supporting electrolyte, a Pt disk electrode, and a calomel reference electrode (SCE). The results are shown in Table II; the complexes exhibit only one redox process with the exception of **1** and **10**, which present two. The analysis of the first wave at scan rates of 50, 100, and 200 mV s^{-1} gives clear evidence that it is an oxidation process for a Rh(I) complex and a reduction one for a Rh(II) complex. Each couple was diffusion-controlled, as evidenced by a constant current function ($i_{p,a}v^{-1/2}$) over the scan rate (from 0.050 to 0.200 V s^{-1}). Values of ΔE_p were in the range expected for fast one-electron couples (see Table II). They are reversible processes for all of them ($i_c/i_a = 1$) except for compound **3** (i_c/i_a = 0.62–0.75, and the function $i_{p,a}v^{-1/2}$ is not constant). The second wave, which is present for complexes **1** and **10**, reveals that there are irreversible redox oxidation processes, probably Rh(II)–Rh(III).

The most significant pairs of complexes are **1**/**5** and **2**/**6**, which have the same ligands but different oxidation states of the metal, so we have compared the oxidation of compound **1**, and its subsequent reduction, with the reduction of **5** and its reoxidation (Figure 1). Although the low solubility of **5** prevents the preparation of 0.50 mM solutions, its cyclic voltammogram indicates that its oxidation and reduction peaks are localized at values identical to those observed for the first redox wave of complex **1**. This behavior is similar to that found for related iridium compounds[9] or for rhodium compounds with the metal in different and accesible oxidation states.[15]

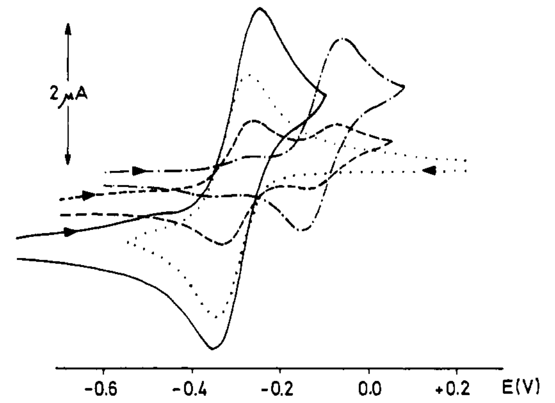

Figure 2. CV scans of $[Rh(C_6Cl_5)_2\{P(OPh)_3\}_2]$ (**6**) (···), $[NBu_4][Rh(C_6Cl_5)_2\{P(OPh)_3\}_2]$ (**2**) (– · –), the product prepared by oxidation of **2** with Cl_2 (- - -), and the product made by substitution of the diolefin in **5** for $P(OPh)_3$ (—) (concentrations ca. 0.50 mM in CH_2Cl_2/0.1 M $[NBu_4][PF_6]$ at ambient temperature; v = 0.10 V s^{-1}; Pt electrode).

Similar behavior was expected for complexes **2** and **6**, and in fact the voltammograms of **2** and of the sample of **6** on which the X-ray crystal diffraction studies were made present only one reversible wave, but the oxidation or reduction peaks are not at the same potential. To explain this, we have performed several cyclic voltammetry measurements on samples of both products obtained from different preparations; Figure 2 shows the results of four voltammograms superimposed: the dotted line is that obtained for *trans*-$[Rh(C_6Cl_5)_2\{P(OPh)_3\}_2]$ (**6**) (same sample on which the X-ray crystal diffraction studies were made), the dotted–dashed line is for $[Bu_4N][Rh(C_6Cl_5)_2\{P(OPh)_3\}_2]$ (**2**), the dashed line is for the product prepared by oxidation of **2** with Cl_2, and the continuous line is for the product made by substitution of the diolefin in **5** for $P(OPh)_3$. This behavior suggests that while **6** crystallizes with a *trans* geometry, **2** is probably the *cis* isomer and its oxidation product is a mixture of both Rh(II) isomers although the *trans* isomer is the main complex.

EPR Studies. The observed EPR spectra measured at room temperature of the seven samples are given by continuous lines in Figure 3. They extend from 220 to 380 mT, and each of them consists of three features, two of which are barely resolved in some cases. In spite of the 100% natural-abundance isotope of rhodium (^{103}Rh has a nuclear spin $I = ^1/_2$), no evidence of hyperfine (HF) structure has been found in all the samples. Consequently, these EPR spectra can be understood only with an electronic Zeeman contribution which turns out to have an orthorhombic symmetry. So the following spin Hamiltonian was used for the spectral description

$$\mathbf{H} = \mu_B(g_x S_x B_x + g_y S_y B_y + g_z S_z B_z)$$

with $S = ^1/_2$; x, y, and z are the principal axes of the $\mathbf{g}$ tensor, and μ_B is the Bohr magneton. Using a Lorentzian

---

(15) Haefner, S. C.; Dunbar, K. R.; Bender C. *J. Am. Chem. Soc.* **1991**, *113*, 9540. Cooper, S. R.; Rawle, S. C.; Yagbasan, R.; Watkin, D. J. *J. Am. Chem. Soc.* **1991**, *113*, 1600.

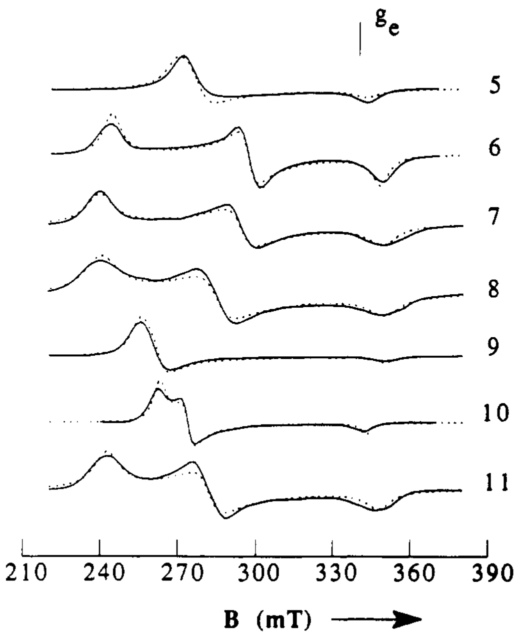

Figure 3. EPR spectra of powdered samples of the rhodium(II) complexes **5**–**11** recorded at room temperature. The continuous lines represent the experimental spectra, and the dotted lines are simulated by using the values given in Table III.

Table III. Principal g Factors and Peak to Peak Width ΔB_{pp} (mT) of the Lorentzian Line Shape Used for Calculating the Simulated Spectra in Figure 3

sample	g_x	g_y	g_z	$g_{av}{}^a$	ΔB_{pp}
5	2.52	2.45	1.99	2.32	7.0
6	2.79	2.29	1.96	2.35	4.5
7	2.84	2.32	1.95	2.37	7.5
8	2.83	2.39	1.95	2.39	9.0
9	2.66	2.59	1.94	2.40	5.0
10	2.58	2.48	1.99	2.35	3.0
11	2.80	2.41	1.96	2.39	7.0

^{a} $g_{av} = (g_x + g_y + g_z)/3$.

line shape with an isotropic peak to peak width (ΔB_{pp}), we have performed simulations of the powder spectra. Good fits of the spectra are achieved for the values collected in Table III. The simulated spectra calculated with these values for g factors and ΔB_{pp} are represented by dotted lines in Figure 3.

These g values can be understood if the unpaired electron is mainly in a d_{z^2} orbital with the z axis perpendicular to the first coordination rhodium plane. This description is similar to that given for some Pt(III) mononuclear compounds[16] and a pair of Ir(II) compounds.[9] In all of them the electronic configuration of the paramagnetic entity is d^7 and the observed g values are in agreement with those calculated for d^7 ions in strong field (low-spin configuration).[17,18] In the present case (electronic configuration of Rh(II) $4d^7$) the g shifts are lower than in those above, which is in agreement with the lower value of the spin–orbit coupling constant for the 4d as compared with the 5d electrons.

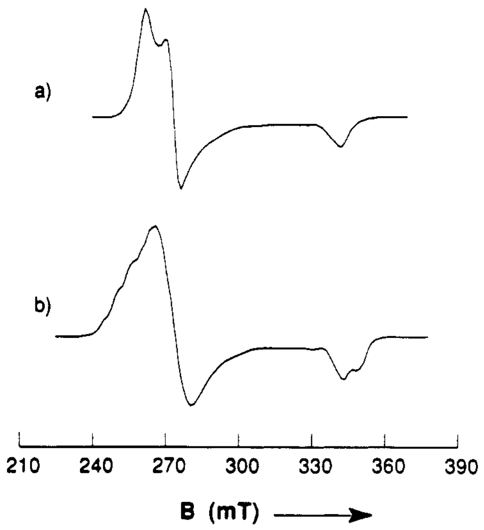

Figure 4. EPR spectra of the rhodium(II) complex **10**: (a) as a powdered sample; (b) in frozen CH_2Cl_2 solution at liquid nitrogen temperature.

In spite of the reasonable agreement between the calculated and experimental spectra, some discrepancies are observed. They are mainly a misfit in the relative intensities and widths of the different features. This can be attributed to the existence of some unresolved hyperfine interaction, which is probably anisotropic, but some additional effects due to an anisotropic width of the resonance lines cannot be discarded. For these reasons we have not analyzed this point thoroughly. Anyhow, an estimation of the isotropic hyperfine constant A following a simple model proposed by Raizaman et al.[18] indicates that the experimental hyperfine splitting, if it takes place, is lower than the predicted one. This points to the existence of some intermolecular interactions, such as exchange, that average toward zero the effective splitting due to hyperfine interaction. This interpretation is corroborated when the spectrum of a frozen solution of compound **10** in dichloromethane is recorded at liquid nitrogen temperature (see Figure 4). The high-field feature consists of two lines 65 mT apart, indicating an effective hyperfine constant along the z axis of about 180 MHz, which is noticeably higher than the upper limit (about 110 MHz) for the solid samples. Otherwise, this EPR spectrum is consistent with the g values measured for the solid sample (Table III).

Molecular Structure of 6. The crystal structure of **6** contains discrete molecules separated by normal van der Waals distances. Figure 5 shows the molecular structure and the numbering scheme of one of the two disordered molecules that form the crystal (see Experimental Section). Atomic coordinates are listed in Table IV, and derived bond distances and angles, in Table V. The structural study confirmed the molecule to be mononuclear. The rhodium location at a crystallographic inversion center originates a centrosymmetric *trans* square planar coordination around the metal. The unique slight distortion from this ideal environment arises from the P(1)–Rh–C(1) bond angle, 92.2(1)°.

The pentachlorophenyl ring bonded to the Rh is roughly planar (maximum deviation 0.010(4) Å), with the Cl atoms slightly out of the ring plane (deviations up to 0.095(1) Å for Cl(6)). This plane is positioned almost perpendicular to the metal coordination plane (dihedral angle 94.9(1)°). The asymmetry of the bond angles around C(1), together with a weak inclination of the C(1)–C(4) vector with respect to the Rh–C(1) bond (2.0(1)°), makes the two Rh···Cl_{ortho}

---

[16] Alonso, P. J.; Alcalá, R.; Usón, R.; Forniés, J. *J. Phys. Chem. Solids* **1991**, *52*, 975.

[17] Lacroix, R. *Helv. Phys. Acta* **1964**, *37*, 627. Maki, A. H.; Edelstein, N.; Davison, A.; Holm, R. H. *J. Am. Chem. Soc.* **1964**, *86*, 4580.

[18] Raizaman, A.; Suss, J. T.; Low, W. *Phys. Rev.* **1977**, *B15*, 5184. Raizaman, A.; Shoenberg, A.; Suss, J. T. *Phys. Rev.* **1979**, *B20*, 1863.

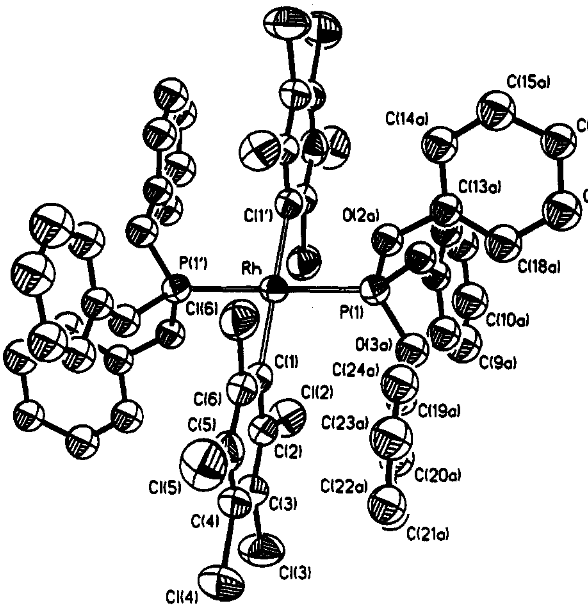

Figure 5. Molecular diagram of [Rh(C_6Cl_5){P(OPh)$_3$}$_2$] (6). Only one disordered "OPh moiety" has been represented (atoms labeled with a). Primed atoms correspond to those related by the symmetry transformation $-x, -y, -z$.

distances different. The shortest one, Rh···Cl(6) = 3.193(1) Å, could be indicative of a feeble metal–halogen interaction: the value of the ρ parameter suggested to characterize this type of interactions is 1.38, in the upper limit of the range described for Ag···X (X = F, Cl) interactions, ρ = 1.21–1.47.[19]

The Rh–C(1) bond distance, 2.080(4) Å, is in the lower part of the range reported for related pentacoordinated pentafluorophenyl-Rh(III) complexes (2.070(5)–2.135(11) Å), where two basal C_6F_5 groups are situated in a relative pseudo-*trans* position;[6,8] but this distance is longer than those observed, in the same compounds, for the apical C_6F_5 ligands, 1.954(15)–2.014(14) Å. If compared with those of related M(II) complexes, this bond separation is analogous to that observed in *trans*-[Rh(2,4,6-$Pr^i_3C_6H_2$)$_2$(tht)$_2$], 2.11(1) Å,[3] or in the Ir(II) complex [Ir(C_6Cl_5)$_2$(cod)], 2.073(5) Å.[9]

The Rh–P(1) length, 2.3000(7) Å, is similar to that reported for the Rh(II) complex [$RhCl_2(PPh_3)_2$], 2.323(2) Å, where two triphenylphosphine ligands are also participating in a square planar coordination in relative *trans* positions.[20]

Experimental Section

General Data. C, H, and N analyses, conductance determinations, and IR and NMR spectroscopy were performed as described elsewhere.[6] MS were recorded in a VG Autospec double-focusing mass spectrometer operating in the negative mode for anionic species and in the positive mode for neutral complexes; ions were produced with the standard Cs^+ gun at ca. 30 kV; 3-nitrobenzyl alcohol (NBA) was used as the matrix. Cyclic voltammetric experiments were performed by employing an EG&G PARC Model 273 potentiostat. A three-electrode system was used, consisting of a platinum disk working electrode, a platinum wire auxiliary electrode, and a saturated calomel reference electrode. The measurements were carried out in CH_2Cl_2 solutions with 0.1 M Bu_4NPF_6 as supporting electrolyte. Under the present experimental conditions, the ferrocenium/ferrocene couple was located at 0.47 V. EPR data were taken in a Varian E-112 spectrometer working in the X-band. The powdered polycrystalline samples were introduced in a standard EPR quartz tube (707-SQ from Wilmad), and their spectra were taken at room temperature. In the case of complex **10**, a solution in dichloromethane was prepared. The magnetic field was measured with an NMR gaussmeter, Bruker ER035M, and the diphenylpicrylhydrazyl (DPPH) resonance signal (g = 2.0037 ± 0.0002) was used for determining the microwave frequencies. The starting rhodium(I) dimers [{Rh(μ-Cl)(L_2)}$_2$] [L_2 = cod,[21] (P(OPh)$_3$)$_2$,[22]

Table IV. Final Atomic Coordinates[a] (×10^4) and Equivalent Isotropic or Isotropic Displacement Coefficients (Å^2 × 10^4) for Complex 6

atom	x/a	y/b	z/c	$U_{eq}{}^b/U_{iso}$
Rh	0	0	0	381(2)
Cl(2)	−1271(1)	1625(1)	−1850(1)	700(5)
Cl(3)	−292(2)	2244(1)	−4035(1)	877(7)
Cl(4)	2139(2)	1439(1)	−4588(1)	884(6)
Cl(5)	3552(1)	−39(1)	−2967(1)	875(6)
Cl(6)	2590(1)	−568(1)	−730(1)	700(5)
P(1)	2063(1)	1807(1)	1252(1)	446(3)
C(1)	637(4)	472(3)	−1452(3)	457(13)
C(2)	39(4)	1116(3)	−2202(3)	477(13)
C(3)	463(4)	1404(3)	−3168(3)	554(15)
C(4)	1546(5)	1049(3)	−3407(3)	583(16)
C(5)	2202(4)	413(3)	−2683(3)	572(15)
C(6)	1747(4)	153(3)	−1713(3)	504(14)
O(1a)	1701(5)	2499(4)	2308(4)	490(11)[c]
C(7a)	761(8)	3153(7)	2277(10)	455(15)
C(8a)	615(11)	3909(11)	1484(9)	599(24)
C(9a)	−239(17)	4605(13)	1585(12)	818(44)
C(10a)	−967(12)	4470(10)	2375(11)	767(31)
C(11a)	−805(11)	3667(10)	3167(8)	641(22)
C(12a)	103(11)	3038(8)	3135(7)	538(18)
O(2a)	3296(5)	1448(4)	2103(4)	448(11)
C(13a)	4435(8)	2183(7)	3215(6)	460(16)
C(14a)	4612(14)	1444(13)	4022(11)	575(38)
C(15a)	5796(11)	2058(11)	5089(9)	632(30)
C(16a)	6661(10)	3397(11)	5388(8)	531(22)
C(17a)	6416(11)	4139(10)	4516(9)	657(25)
C(18a)	5248(9)	3494(7)	3415(7)	597(18)
O(3a)	2939(5)	3001(4)	838(4)	520(12)
C(19a)	3763(8)	3092(7)	44(6)	442(16)
C(20a)	3373(12)	3605(10)	−861(9)	561(32)
C(21a)	4274(13)	3780(9)	−1612(8)	608(25)
C(22a)	5499(11)	3428(9)	−1463(9)	591(19)
C(23a)	5800(12)	2899(10)	−516(11)	727(24)
C(24a)	4978(11)	2729(7)	268(7)	589(19)
O(1b)	1928(5)	3130(5)	1372(4)	529(13)
C(7b)	923(8)	3423(9)	1834(9)	479(17)
C(8b)	366(12)	4206(11)	1343(9)	640(30)
C(9b)	−587(15)	4525(12)	1726(12)	670(35)
C(10b)	−1003(10)	4172(11)	2700(10)	612(24)
C(11b)	−383(15)	3348(12)	3209(9)	717(25)
C(12b)	585(11)	3007(8)	2794(11)	618(22)
O(2b)	2698(6)	1594(5)	2480(4)	524(12)
C(13b)	4111(9)	2349(8)	3406(7)	501(19)
C(14b)	4750(13)	1718(12)	4106(11)	508(37)
C(15b)	6064(14)	2467(14)	5145(10)	692(32)
C(16b)	6701(14)	3783(12)	5297(11)	741(36)
C(17b)	6078(14)	4289(12)	4646(10)	784(32)
C(18b)	4787(10)	3636(9)	3685(8)	676(22)
O(3b)	3729(5)	2359(5)	968(4)	552(13)
C(19b)	4177(10)	2824(7)	54(6)	441(16)
C(20b)	3475(13)	3456(11)	−631(11)	572(33)
C(21b)	3886(11)	3902(9)	−1556(8)	552(26)
C(22b)	5118(11)	3710(8)	−1716(7)	537(20)
C(23b)	5875(11)	3139(10)	−1016(12)	669(23)
C(24b)	5421(12)	2686(9)	−112(10)	676(24)

[a] Atoms labeled a or b correspond to the two disordered "(OPh)$_3$ moieties". [b] Equivalent isotropic U defined as one-third of the trace of the orthogonalized U_{ij} tensor. [c] From this atom downward, isotropic thermal parameters are expressed.

---

(19) Usón, R.; Forniés, J.; Tomás, M. *J. Organomet. Chem.* **1988**, *358*, 525.

(20) Ogle, C. A.; Masterman, T. C.; Hubbard, J. L. *J. Chem. Soc., Chem. Commun.* **1990**, 1733.

(21) Giordano, G.; Crabtree, R. H. *Inorg. Synth.* **1979**, *19*, 218.

Table V. Selected Bond Distances (Å) and Angles (deg) for Complex 6

Rh–P(1)	2.3000(7)	Rh–C(1)	2.080(4)
P(1)–O(1a)	1.644(5)	P(1)–O(1b)	1.599(6)
P(1)–O(2a)	1.586(5)	P(1)–O(2b)	1.535(5)
P(1)–O(3a)	1.544(5)	P(1)–O(3b)	1.664(5)
O(1a)–C(7a)	1.407(11)	O(1b)–C(7b)	1.395(12)
O(2a)–C(13a)	1.425(7)	O(2b)–C(13b)	1.412(8)
O(3a)–C(19a)	1.410(10)	O(3b)–C(19b)	1.385(10)
C–C(C_6Cl_5) mean	1.383(3)	C–Cl mean	1.728(2)
P(1)–Rh–C(1)	92.2(1)	P(1)–Rh–C(1′)[a]	87.8(1)
Rh–P(1)–O(1a)	115.7(2)	Rh–P(1)–O(1b)	119.8(2)
Rh–P(1)–O(2a)	110.5(2)	Rh–P(1)–O(2b)	112.5(2)
Rh–P(1)–O(3a)	123.5(2)	Rh–P(1)–O(3b)	118.5(2)
P(1)–O(1a)–C(7a)	131.3(5)	P(1)–O(1b)–C(7b)	126.5(5)
P(1)–O(2a)–C(13a)	127.9(4)	P(1)–O(2b)–C(13b)	130.0(5)
P(1)–O(3a)–C(19a)	127.8(5)	P(1)–O(3b)–C(19b)	135.0(5)
C(1)–C(2)–C(3)	123.6(4)	C(1)–C(6)–C(5)	122.9(4)
C(1)–C(2)–Cl(2)	117.0(3)	C(1)–C(6)–Cl(6)	116.0(3)
C(3)–C(2)–Cl(2)	119.3(3)	C(5)–C(6)–Cl(6)	121.1(3)
Rh–C(1)–C(2)	124.6(3)	Rh–C(1)–C(6)	119.8(2)
C(2)–C(1)–C(6)	115.6(3)		

[a] Primed atom is related to the unprimed one by the symmetry operation $-x,-y,-z$.

$(CO)_2$,[23] $(CO)(PPh_3)$[24]] were prepared as described in the literature. LiC_6Cl_5 was obtained as described in ref 25 and was directly used without further isolation. Diethyl ether, THF, CH_2Cl_2, and hexane were distilled under nitrogen from the appropriate drying agents.

Synthesis of $[NBu_4][Rh(C_6Cl_5)_2(L_2)]$ [L_2: 1,5-Cyclooctadiene (cod), 1; $(P(OPh)_3)_2$, 2; $(CO)_2$, 3; $(CO)(PPh_3)$, 4]. Solid rhodium(I) dimers $[\{Rh(\mu\text{-}Cl)(L_2)\}_2]$ (0.2–0.5 mmol) were added to diethyl ether solutions of LiC_6Cl_5 (1.0–2.5 mmol) at −50 °C. Each mixture was allowed to warm slowly to room temperature while stirring was continued for 4 h; during this time the starting rhodium complexes were dissolving and new oily solids were forming in all the cases but 3, which gave a brown solution. For complexes 1, 2, and 4, the extraction and purification were as follows: the supernatant solutions were separated from the solids by decantation; the solid residues were washed twice with 20 mL of aqueous diethyl ether and treated with a solution of NBu_4Br (Rh:salt = 1:1) in methanol (10 mL), yielding complexes 1, 2, and 4 as crystalline solids (yields: 62% 1, 50% 2, 48% 4). For compound 3, the brown solution was treated with aqueous diethyl ether (20 mL) to destroy excess LiC_6Cl_5, and the solution was evaporated to dryness. The residue was extracted with CH_2Cl_2 (30 mL), and the extract was filtered through Kieselguhr under a nitrogen atmosphere. Addition of NBu_4Br, concentration to ca. 5 mL, and treatment with a mixture of propan-2-ol/hexane (4:20 mL) caused crystallization of 3 as a yellow solid (52% yield).

1: ^1H NMR ($CDCl_3$) δ 3.2 (m, 4H, =CH), 2.4 (m, 8H, CH_2); ^{13}C NMR ($CDCl_3$) δ 138.6, 127.3, 122.9 (s, C_{ortho}, C_{para}, C_{meta}), 81.8 (s, =CH, cod), 31.2 (s, CH_2, cod), 59.0, 23.7, 19.6, 13.5 (s, NBu_4); MS (FAB) *m/e* 709 (M: $[Rh(C_6Cl_5)_2(cod)]^-$, 67), 601 (M − cod, 61), 460 (M − C_6Cl_5, 16), 352 (M − cod − C_6Cl_5, 93).

2: ^{31}P NMR ($CDCl_3$) δ 122.7 (d, J_{PRh} = 239.1 Hz); ^{13}C NMR ($CDCl_3$, −50 °C) δ 140.9, 128.7, 126.5 (s, C_{ortho}, C_{para}, C_{meta}, C_6Cl_5), 151.9, 128.2, 122.5, 120.4 (s, C_{ipso}, C_{ortho}, C_{para}, C_{meta} $P(OPh_3)$), 59.0, 23.7, 19.6, 13.5 (s, NBu_4); MS (FAB) *m/e* 1220 (M: $[Rh(C_6Cl_5)_2\{P(OPh)_3\}_2]^-$, 24), 601 (M − $\{P(OPh)_3\}_2$, 100), 352 (M − C_6Cl_5 − $\{P(OPh)_3\}_2$, 12).

3: IR (Nujol) ν_{CO} 2030, 1960 cm^{-1}; ^{13}C NMR ($CDCl_3$) δ 191.2 (d, J_{CRh} = 59 Hz, CO), 168.6 (d, J_{CRh} = 37 Hz, C_{ipso}), 140.6, 128.0, 126.6 (s, C_{ortho}, C_{para}, C_{meta}), 59.0, 23.7, 19.6, 13.5 (s, NBu_4); MS (FAB) *m/e* 656 (M: $[Rh(C_6Cl_5)(CO)_2]^-$, 100), 601 (M − $(CO)_2$, 96), 352 ($Rh(C_6Cl_5)$, 15).

Table VI. Crystallographic Data for 6

Crystal Data	
formula	$C_{48}H_{30}Cl_{10}O_6P_2Rh$
mol wt	1222.14
color and habit	red, transparent, prismatic block
cryst size, mm	0.140 × 0.380 × 0.798
cryst syst	triclinic
space group	$P\bar{1}$
a, Å	9.8718(9)
b, Å	11.6830(13)
c, Å	12.1366(12)
α, deg	95.465(6)
β, deg	105.824(4)
γ, deg	112.738(5)
V, Å^3; Z	1209.9(2); 1
D_{calcd}, g·cm^{-3}	1.677
Data Collection and Refinement	
diffractometer	4-circle, Siemens AED
λ(Mo Kα), Å; technique	0.710 69; bisecting geometry
monochromator	graphite oriented
μ, cm^{-1}	10.18
scan type	$\omega/2\theta$
2θ range, deg	3–50
no. of data collected	5275
no. of unique data	4261
unique obs data	3889, $F_o \geq 5\sigma(F_o)$
no. of params refined	286
R, R_w[a]	0.0407, 0.0481
max, min transm factors	0.6368, 0.8722

[a] $w^{-1} = \sigma^2(F_o) + 0.000508F_o^2$.

4: IR (Nujol) ν_{CO} 1945 cm^{-1}; ^{31}P NMR ($CDCl_3$) δ 40.1 (d, J_{PRh} = 131.3 Hz); ^{13}C NMR ($CDCl_3$) δ 195.1 (dd, J_{CRh} = 62 Hz, J_{CP} = 14 Hz, CO), 181.4 (dd, J_{CRh} = 35 Hz, J_{CP} = 16 Hz, C_{ipso}, C_6Cl_5), 176.4 (dd, J_{CRh} = 40 Hz, J_{CP} = 83 Hz, C_{ipso}, C_6Cl_5).

Preparation of $[Rh(C_6Cl_5)_2(cod)]$ (5). To a solution of compound 1 (0.100 g, 0.105 mmol) in 10 mL of CH_2Cl_2 was added very slowly a solution of Cl_2 (0.595 N) (0.18 mL, 0.105 mmol) in the same solvent. A pink solid formed; after 10 min of stirring, the solid, 5, was filtered off and washed with methanol (5 mL) and diethyl ether (5 mL) (62% yield).

Preparation of $[Rh(C_6Cl_5)_2\{P(OPh)_3\}_2]$ (6). A CH_2Cl_2 solution of Cl_2 (0.595 N) (0.12 mL, 0.07 mmol) was slowly added to a light orange solution of 2 (100 mg, 0.07 mmol). The color of the solution changed to red immediately; after 10 min of stirring, the solution was concentrated to 1 mL, and 15 mL of MeOH was added; the resulting precipitate, 6, was filtered off and washed with methanol (5 mL) and diethyl ether (5 mL) (48% yield): MS (FAB) *m/e* 1222 (M, 25), 912 (M − $P(OPh)_3$, 57), 601 (M − $\{P(OPh)_3\}_2$, 49).

Preparation of $[Rh(C_6Cl_5)_2L_2]$ (6–11). To suspensions of 5 (0.05 g, 0.07 mmol) in CH_2Cl_2 (10 mL) were added neutral ligands. Their quantities and the reaction times were as follows: $P(OPh)_3$, 0.036 g, 0.14 mmol, 8 h; $P(OMe)_3$, 0.165 mL, 0.14 mmol, 6 h; PPh_3, 0.037 g, 0.14 mmol, 12 h; py, 0.0113 mL, 0.14 mmol, 2 h; dpe, 0.028 g, 0.07 mmol, 24 h; dpm, 0.027 g, 0.07 mmol, 18 h. The solids dissolved during the reactions, and the resulting solutions were concentrated to 1 mL; the addition of MeOH (5 mL) caused the precipitation of the complexes as microcrystalline solids, which were filtered off and washed with MeOH. MS (FAB): 7, *m/e* 725 (M − $P(OMe)_3$, 8); 8, *m/e* 1125 (M, 100), 863 (M − PPh_3, 89), 613 (M − PPh_3 − C_6Cl_5, 90); 9, *m/e* 680 (M − py, 27); 10, *m/e* 999 (M, 99), 750 (M − dpe, 27), 501 (M − $(C_6Cl_5)_2$, 51); 11, *m/e* 985 (M, 96), 736 (M − C_6Cl_5, 21), 487 (M − $(C_6Cl_5)_2$, 100).

X-ray Structure Analysis of 6. *Collection and Reduction of Data.* Crystals suitable for X-ray study were obtained by slow evaporation of a CH_2Cl_2 solution of 6. A dark pink prismatic crystal was glued on a glass fiber and mounted on a Siemens AED-2 diffractometer. A summary of crystal data, intensity collection procedures, and refinement data is reported in Table VI. Cell constants were obtained from the least-squares fit of the setting angles of 70 reflections in the range $20 \leq 2\theta \leq 45°$. The 5275 recorded reflections ($\pm h,\pm k,-l$) were corrected for Lorentz and polarization effects. Three orientation and intensity

---

[22] Haines, L. M. *Inorg. Chem.* **1970**, *9*, 1517.

[23] Powell, J.; Shaw, B. L. *J. Chem. Soc. A* **1968**, 211.

[24] Steele, D. F.; Stephenson, T. A. *J. Chem. Soc. A* **1972**, 2161.

[25] Rausch, M. D.; Moser, G. A.; Meade, C. F. *J. Organomet. Chem.* **1973**, *51*, 1.

standards were monitored every 55 min of measuring time; no intensity decay was observed. A numerical method based on crystal morphological faces was used to correct for absorption effects.[26]

Structure Solution and Refinement. The structure was solved by Patterson (Rh atom) and conventional Fourier techniques. Refinement was carried out by full-matrix least-squares procedures with initial isotropic thermal parameters. At this stage, several intense residual peaks were observed around the OPh groups together with unusual thermal parameters for the included atoms of these groups. These data were indicative of a situation of ligand disorder involving the three independent OC_6H_5 moieties. A disorder model was built based on the presence of two different "$(OPh)_3$ moieties" which were refined with complementary occupancy factors (0.514(4)). Further refinement was performed with anisotropic thermal parameters for all non-hydrogen and non-disordered atoms of the molecule. Hydrogen atoms were included in calculated positions and refined riding on carbon atoms with a common isotropic thermal parameter. The function minimized was $\sum(|F_o| - |F_c|)^2$ with the weight defined as $w^{-1} = \sigma^2(F_o) + 0.000508F_o^2$. Atomic scattering factors, corrected for anomalous dispersion for Rh, P, and Cl, were taken from ref 27. Final R and R_w values were 0.041 and 0.048, respectively. All calculations were performed by use of the SHELXTL-PLUS system of computer programs.[28]

Acknowledgment. We thank the DGICYT (Dirección General de Investigación Científica y Técnica) for finanical support (Project PB 88 0386).

Supplementary Material Available: Tables of anisotropic thermal parameters, hydrogen coordinates, experimental details of the X-ray study, bond distances and angles, selected least-squares planes, and interatomic distances (19 pages). Ordering information is given on any current masthead page.

OM9301187

---

[26] Busing, W. R.; Levy, H. A. *Acta Crystallogr.* 1957, *10*, 180.

[27] *International Tables for X-Ray Crystallography*; Kynoch Press: Birmingham, England, 1974; Vol. 4.

[28] *SHELXTL PLUS Program for Crystal Structure Determinations*; Siemens Analytical X-Ray Instruments: Madison, WI, 1990.